GEOPHYSICAL RESEARCH LETTERS, VOL. 36, L18607, doi:10.1029/2009GL039120, 2009

Behavior of the Wyrtki Jet observed with surface drifting buoys and satellite altimeter

Yun Qiu,[1] Li Li,[1] and Weidong Yu[2]

Received 10 May 2009; revised 9 July 2009; accepted 14 August 2009; published 22 September 2009.

[1] Analyses of up-to-date data from satellite-tracked surface drifters indicate that the Wyrtki Jets (WJ) of the equatorial Indian Ocean (EIO) are developed firstly in the central EIO between 75°E and 80°E and then propagate westward along the equator at speeds of about 0.7 m s^{-1}. Climatologically, the fall jet is both stronger and wider than its spring counterpart. This westward propagation phenomenon is supported by altimetry observation. It is suggested that the westward propagation of the jets in the western EIO (55°–75°E) is primarily forced directly by the westward propagating zonal winds. Whereas in the eastern EIO (east to 80°E), propagation of the jet signals is ambiguous although the zonal wind pattern is observed moving east. It is also evident that the WJs are subject to strong interannual variability, which may associate with El Niño/Southern Oscillation (ENSO) and Indian Ocean Dipole (IOD). **Citation:** Qiu, Y., L. Li, and W. Yu (2009), Behavior of the Wyrtki Jet observed with surface drifting buoys and satellite altimeter, *Geophys. Res. Lett.*, *36*, L18607, doi:10.1029/2009GL039120.

1. Introduction

[2] The WJ is a unique phenomenon in the EIO, which is an intense and narrow eastward surface current occurring twice a year during the monsoon transition periods in spring and fall [*Wyrtki*, 1973]. It is suggested that the jet is wind-driven since its occurrence coincides with the onsets of biannual westerly along the equator [*Wyrtki*, 1973; *Wunsch*, 1977; *Han et al.*, 1999]. The jets advect both heat and salt towards east and thereby change the upper ocean heat and salt budgets [*Wyrtki*, 1973; *Murtugudde and Busalacchi*, 1999; *Masson et al.*, 2002], which have significant impacts on the large-scale air-sea interactions in the Indian Ocean basin.

[3] The dynamics of the WJ has been studied by a number of numerical simulations [e.g., *O'Brien and Hurlburt*, 1974; *Cane*, 1980; *Reverdin*, 1987; *Jensen*, 1993; *Han et al.*, 2004]. It is believed that direct wind forcing is the dominant mechanism of the WJs, though the effects of reflected Rossby waves, resonance, and mixing layer shear are also important [*Han et al.*, 1999; *Schott and McCreary*, 2001; *Yuan and Han*, 2006].

[4] The first comprehensive field observation on the WJ was conducted in ocean area near Gan Island (0°41′S, 73°10′E) [*Knox*, 1976]. The result further confirmed the domination of direct wind forcing and revealed the importance of remote forcing induced by propagating equatorial waves [*Knox*, 1976; *McPhaden*, 1982]. Since then, a number of observational studies were achieved with drifters [*Luyten et al.*, 1980; *Reverdin*, 1985; *Molinari et al.*, 1990; *Grodsky et al.*, 2001], moorings [*Reppin et al.*, 1999; *Nagura and McPhaden*, 2008], and satellite remote sensing [*Grodsky et al.*, 2001]. Even though, much has still to be learnt about the WJ. For example, large discrepancies were found in different studies concerning the relative strengths of the two jets [*Schott and McCreary*, 2001].

[5] With the accumulation of the surface drifter data and the availability of altimeter data, it is now possible to compile an observational image of the WJs in detail. In this paper, we first present a WJ climatology derived from up-to-date observations of satellite-tracked surface drifter. Time series representing the jets were then constructed from satellite altimetry. Finally, wind-driven nature of the WJs and their variability were explored through time series analysis.

2. Data

[6] The SVP (Surface Velocity Program) drifter data used in this study include 6-hour interpolated and wind-corrected current velocity, drifter's position, and surface wind from NCEP/NCAR reanalysis interpolated to drifters' location [*Niiler et al.*, 2003]. Most SVP drifters have their drogues tethered at 15 m depth to measure mixed layer currents. In our study, data from a total of 305 drifters were used to construct the WJ climatology and the associated wind field (Figure 1).

[7] The CLS (Collecte Localisation Satellites) sea level anomaly (SLA) files merged from TOPEX/Poseidon and ERS [*Ducet et al.*, 2000] is available at a 7-day interval with a 1/3° Mercator Grid for the period from October 14, 1992 to May 8, 2002. In our analyses, high-frequency signals were removed by a 90-day low-pass filter. A subset of weekly 1° × 1° gridded ERS wind data from October 1992 to January 2001 were used in the time series analyses.

3. Wyrtki Jet Climatology

[8] The WJ climatology derived from SVP surface drifting buoys is shown in Figure 1. In the latitudinal view (Figure 1a), the WJs, characterized by eastward currents over 0.5 m s^{-1} in their cores, is quite remarkable. The jets occur twice a year with peaks appearing in April and November, inducing a strongly semiannual signal around the equator. Beyond that, the semiannual signal weakens, and the annual signal becomes dominated. Comparatively,

[1]Third Institute of Oceanography, State Oceanic Administration, Xiamen, China.
[2]First Institute of Oceanography, State Oceanic Administration, Qingdao, China.

0094-8276/09/2009GL039120$05.00

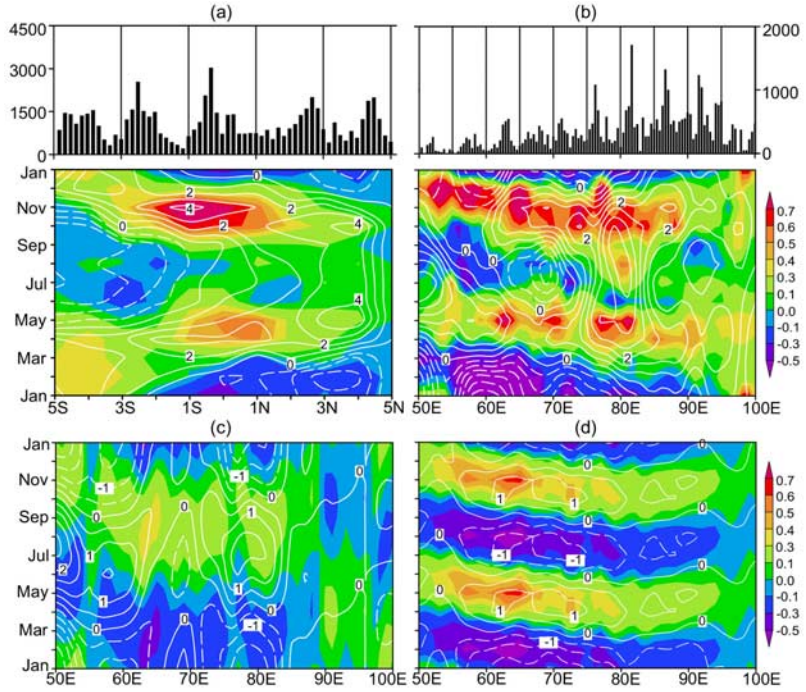

Figure 1. Annual evolution of (a) zonal surface current (colors, in m s^{-1}) and zonal wind speed (overlapped contours, in m s^{-1}) in the EIO averaged from 60°E to 90°E along with the monthly statistics of available drifter measurement (top) in each two degree latitudinal bin; (b) zonal surface current and wind averaged from 2°S to 2°N, and (c) their annual and (d) semiannual components. The monthly statistics of available drifter measurement in each 5° longitudinal bin is also shown (Figure 1b, top).

the fall jet is stronger (~0.7 m s^{-1}) than its spring counterpart (~0.5 m s^{-1}), and is also broader in scale (3°S–2°N vs. 1°S–1.5°N). Unlike the spring jet being symmetrical about the equator, the fall counterpart deflects southward from the equator with its core at about 1°S. This may largely be caused by the mean currents, which also presents an eastward maximum at 1°S (not shown). The pattern of zonal wind overlapped (Figure 1a) are extremely similar to the zonal current, indicating that occurrence of the jets is concurrent with the onset of strong westerly over the EIO (Figure 1) and suggesting a wind-driven nature of the WJs in the climatological sense.

[9] The annual signal becomes dominant beyond the WJ region, which reflects the influences from the Equatorial Counter Current (ECC) and the Indian Monsoon Drift (IMD). South to 2°S, the ECC flows westward from June through October, and becomes eastward in rest months. North to 2°N, in contrast, IMD flows eastward from May to November and reverses direction in other months [*Schott and McCreary*, 2001].

[10] Longitudinally, both the spring and fall jets extend across the EIO inducing the dominant semiannual signals in the whole equatorial region (Figure 1b). The semiannual component (Figure 1d) explains ~68% variance of the zonal current, and is more than twice the variance of the annual component (Figure 1c), even though the annual wind component is in fact more powerful in areas near the western boundary and south to the Indian subcontinent around 80°E.

[11] An important fact revealed here is that both the spring and the fall jets emerge first in the domain of 75°–80°E. And, from there, a westward phase shift is clearly visible as noted earlier by *Molinari et al.* [1990]. A gross estimation suggests a general propagation speed of ~0.7 m s^{-1}. An eastward phase lag, although not as clear, may also be seen in the eastern EIO, which suggests a faster eastward phase speed over 1 m s^{-1}.

[12] It is also noted that the year round evolutional pattern of semiannual winds are extremely similar to that of the zonal current (Figure 1d). This high coherency strongly suggests that in addition to generation of the jets, local wind forcing may also be responsible for the observed phase shift of the semiannual jet signal.

4. WJs Observed With Satellite Altimetry

[13] Previous studies have shown that the WJ was in mainly geostrophic balance [*O'Brien and Hurlburt*, 1974]. Hence, the zonal component of geostrophic velocity can be expressed as

$$u = -\frac{g}{f}\frac{\partial \eta}{\partial y} = -\frac{g}{f}\frac{\partial(\overline{\eta} + \eta')}{\partial y}, \tag{1}$$

here g denotes the gravity constant, f the Coriolis parameter, $\overline{\eta}$ and η' the mean and anomaly of sea level respectively. Assuming there is no geostrophic mean current in the EIO, and then we have

$$u = -\frac{g}{f}\frac{\partial \eta'}{\partial y}. \tag{2}$$

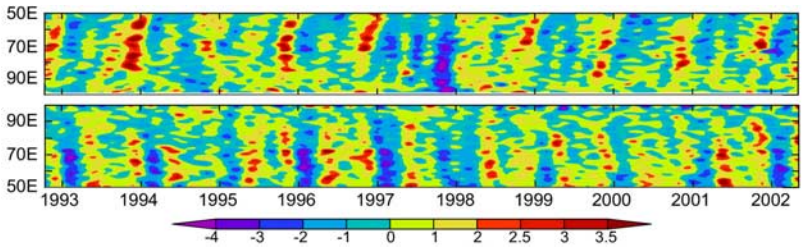

Figure 2. Time-longitude plots of meridional sea level gradients (ΔSLA, in cm) immediately (top) north (ΔSLA_n) and (bottom) south (ΔSLA_s) to the equator in the Indian Ocean showing strong semiannual eastward WJs (positive ΔSLA) and their interannual and spatial variability.

Thus, the meridian SLA differences north ($\Delta SLA_n = SLA_{0.5°N} - SLA_{1.5°N}$) and south ($\Delta SLA_s = SLA_{0.5°S} - SLA_{1.5°S}$) of the equator derived from satellite altimetry can be taken as a proxy of the WJ strength on each side of the equator with positive ΔSLA denoting eastward flow, which allow a quantitative estimate to the jets and their variability [*Masson et al.*, 2003].

[14] The sea level slopes, ΔSLA, on both sides immediately off the equator derived from satellite altimetry from 1992 to 2002 are presented in Figure 2, in which the main features of the WJs are well documented further. Twice a year, eastward currents (positive ΔSLA denoted by warm colors), are observed regularly during spring and autumn on either side of the equator for the whole period except in 1997. The eastward-flowing jet signals are quite obvious between 55°E and 80°E, which generally emerge at around 80°E first and propagate westward along the equator toward the Africa coast. Similar to the climatology (Figure 1b), the semiannual signal becomes difficult to identify east to 80°E, presumably due to interfering with variability of other timescales [*Masson et al.*, 2002; *Masumoto et al.*, 2005]. West to 55°E, the propagating signals are also destroyed because of the strong, seasonally altering currents [*Schott and McCreary*, 2001] and planetary wave interaction [*Yuan and Han*, 2006] near the western boundary. The above altimetry derived features are well consistent with the climatology and assure ΔSLA s a reasonable measure of the WJs.

[15] A worth noting feature revealed by Figure 2 is the differences across the equator. It appears that, north of the equator, the fall jet is always more intense than the spring one, whereas to the south, strengths of the WJs are more evenly distributed in a year. Hence, the semiannual jet signal is much clearer in the south, and the difference of strength between spring and fall (Figure 1) is caused mainly by the northern component of the WJ. An additional difference between the two components was observed near the western boundary, where the westward propagating WJ can reach almost 50°E in the north, but the propagation is hard to see west to 60°E in the south.

[16] It is also revealed by Figure 2 that, in addition to semiannual variation, the WJ exhibits prominent interannual variability as well. The fall WJ in 1994 is weak and can only be seen west to 70°E. More dramatic changes were observed in 1997, when the semiannual jet cycle collapsed totally and negative slopes were detected in fall while the WJ is expected. Previous studies have indicated that anomaly easterly wind events over EIO associated with ENSO and IOD should account for these changes [*Vinayachandran et al.*, 1999; *Grodsky et al.*, 2001; *Cai et al.*, 2005; *Nagura and McPhaden*, 2008]. This interannual variability may also explain the large discrepancies in their relative strength observed during different periods [*Knox*, 1976; *McPhaden*, 1982; *Molinari et al.*, 1990; *Donguy and Meyers*, 1995].

5. Zonal Wind Forcing

[17] It has long been suggested that the WJs are mainly forced by the equatorial westerlies between the two monsoons [*Wyrtki*, 1973], which were argued later with models and with observations of relatively short time spans (see *Han et al.* [1999] for details). Since ΔSLA provides a measure to the strength of the WJs, we can now examine this driving mechanism with long time series for the first time.

[18] Results of the time series analyses show that power spectra of ΔSLA, and hence the WJs, have an unique and outstanding peak between 55°E and 80°E (Figure 3a),

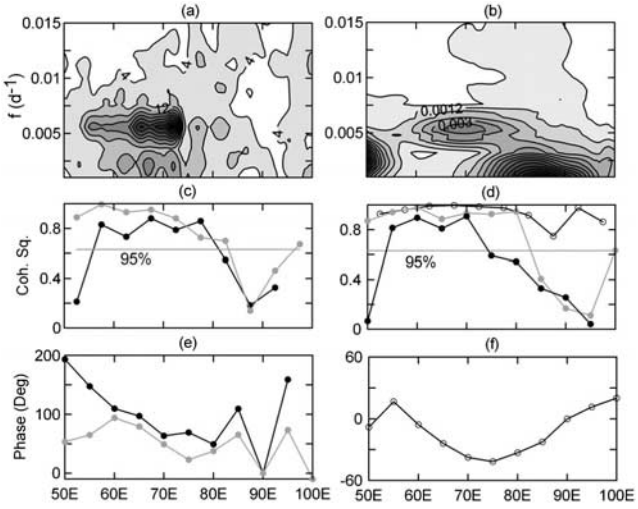

Figure 3. Results of time series analysis showing longitude-frequency distribution of power spectra density of (a) $\overline{\Delta SLA} = 1/2(\Delta SLA_n + \Delta SLA_s)$ and (b) equatorial zonal wind stress averaged from 1.5°S to 1.5°N; coherences between neighboring points in the semiannual band for (c) ΔSLA s and (d) zonal winds (open circle); and (e and f) their phases referred to 90°E. Also shown in Figure 3d is the local coherence between ΔSLA and zonal wind stress. Dark (light) lines with solid circle indicate that of ΔSLA_n (ΔSLA_s).

which coincides with the semiannual peak in the spectra of equatorial zonal wind (Figure 3b) and appears to be the dominated geostrophic signal in the EIO. It is thus suggested that the WJs be most energetic there and likely be generated mainly by semiannual winds in the western interior EIO (wiEIO). It is also noted that, in addition to the semiannual fluctuation, there are also two stronger maxima around the annual band (Figure 3b): one near the western boundary associated with the monsoon winds off Somalia [*Schott and McCreary*, 2001]; the other centered near 82°E, due to the Indian monsoon winds extending southward from the Bay of Bengal [*Han et al.*, 1999]. Despite the energetic annual winds in the eastern EIO and near the western boundary (Figures 1c and 3b), no corresponding annual geostrophic response was observed from ΔSLA, however.

[19] The wind-forced mechanism of the WJs was further investigated with cross-spectral analyses. At the semiannual band, ΔSLA s of the neighboring points are coherent above the 95% significant level on either side (north and south) of the equator in the wiEIO (Figure 3c), and a westward phase shift is clearly presented (Figure 3e) indicating a westward propagating speed around 0.6 m s^{-1} (55°–80°E for ΔSLA_n and 60°–80°E for ΔSLA_s), consistent with what derived from surface drifters. Beyond that region, the coherence (Figure 3c) is generally below the 95% significant level and the phase (Figure 3e) insignificant.

[20] Comparatively, semiannual zonal winds are highly coherent throughout the EIO, especially between 55°E and 80°E (Figure 3d, open circles). The phase relationship (Figure 3f) indicates that they generally emerge between 70°E and 75°E near Maldives first, and then propagate along the equator in both directions with phase speeds around 0.7 m s^{-1} westward and over 1.0 m s^{-1} eastward. Note that the westward propagating regime of zonal wind in the wiEIO matches quite well with that of the ΔSLA s (Figure 3e). Besides, their propagating speeds are close to each other. From phase distribution of the zonal wind stress for semiannual band (Figure 3f), the zonal wind pattern do move in such a way as to force the observed propagation of zonal currents, which corroborates the dominant forcing of local wind on the westward propagation of the jets in the wiEIO.

[21] Finally and most convincingly, the local coherences of ΔSLA with zonal wind were highly significant above the 95% level in the wiEIO area west to 80°E in the south (Figure 3d, light curve with solid dots) and from 55°E to 75°E in the north (Figure 3d, dark curve with solid dots). It is thus concluded that the WJs are mainly generated by semiannual zonal winds over the wiEIO, where the jet signal propagates westward following the translating wind field. Besides, the westward propagating Rossby waves near the equator may collaborate or even resonate with the wind forced jets as suggested by *Jensen* [1993] and *Han et al.* [1999], and play a role on their propagation.

[22] Unlike the wiEIO, in the western boundary area and the eastern basin (east to 80°E), results of the time series analyses suggest that direct wind forcing is not dominant anymore, where their coherence with ΔSLA is low (Figure 3d, solid dots). Particularly in the eastern basins, the zonal wind signal is observed moving eastward coherently (Figures 3d and 3f), but no coherent propagation of the WJs was observed (Figures 3c and 3e). A blend of the additional influence from wave reflections at both the eastern and western boundary [*Han et al.*, 1999; *Le Blanc and Boulanger*, 2001; *Yuan and Han*, 2006], and from the salinity induced barrier layer in the eastern EIO [*Masson et al.*, 2003], may greatly reduce the coherence between wind and current. A quantification of the relative importance of these different forcing factors awaits further investigation.

6. Conclusions

[23] The behavior of the Wyrtki Jet was investigated with observations from surface drifting buoys and satellite altimeter. The results indicate that the WJs are developed primarily in the western EIO from 55°–80°E, where the semiannual zonal winds are most energetic, and are driven mainly by the direct forcing of local zonal winds. Twice a year in April and October, the jets emerge initially in the central EIO (between 75°–80°E) right after the onsets of equatorial westerlies there, which then propagate westward coherently in the western EIO. The westward propagation is predominantly caused by the westward migrating of the semiannual wind pattern along the equator.

[24] In contrast, despite the eastward migration of the semiannual zonal wind stress, propagation of the jet signals is ambiguous in the eastern EIO. Reflection of equatorial waves near boundaries and profound barrier layers in the eastern EIO are likely to reduce the coherence between wind and current.

[25] The analyses also revealed several differences between the two jets. It was shown that, climatologically, the fall WJ is stronger (~0.7 m s^{-1}) than its spring counterpart (~0.5 cm s^{-1}), and that the core of the fall jet is deflected southward to 1°S, whereas the spring jet is centered at the equator. It is also evident the WJs are subject to variability associated with strong interannual events like ENSO and IOD, which may occasionally alter the climatological patterns of the WJs.

[26] **Acknowledgments.** We would like to thank N. A. Maximenko for kindly providing the drifter data. The SLA data were produced by Ssalto/Duacs and distributed by Aviso, with support from Cnes, and the ERS wind data were obtained from CERSAT, at IFREMER, Plouzané, France. Comments given by Quanan Zheng and two anonymous reviewers are highly appreciated. This research was supported by the Chinese Ministry of Science and Technology through the National Basic Research Program (grant 2009CB421205), and by the National Natural Science Foundation of China (grant 40806014).

References

Cai, W., G. Meyers, and G. Shi (2005), Transmission of ENSO signal to the Indian Ocean, *Geophys. Res. Lett.*, *32*, L05616, doi:10.1029/2004GL021736.

Cane, M. A. (1980), On the dynamics of equatorial currents, with application to the Indian Ocean, *Deep Sea Res., Part I*, *27*(7), 525–544, doi:10.1016/0198-0149(80)90038-2.

Donguy, J. R., and G. Meyers (1995), Observations of geostrophic transport variability in the western tropical Indian Ocean, *Deep Sea Res., Part I*, *42*(6), 1007–1028, doi:10.1016/0967-0637(95)00047-A.

Ducet, N., P. Y. Le Traon, and G. Reverdin (2000), Global high-resolution mapping of ocean circulation from TOPEX/Poseidon and ERS-1 and -2, *J. Geophys. Res.*, *105*(C8), 19,477–19,498, doi:10.1029/2000JC900063.

Grodsky, S. A., J. A. Carton, and R. Murtugudde (2001), Anomalous surface currents in the tropical Indian Ocean, *Geophys. Res. Lett.*, *28*(22), 4207–4210, doi:10.1029/2001GL013592.

Han, W. Q., J. P. McCreary Jr., D. L. T. Anderson, and A. J. Mariano (1999), Dynamics of the eastern surface jets in the equatorial Indian

Ocean, *J. Phys. Oceanogr.*, *29*(9), 2191–2209, doi:10.1175/1520-0485(1999)029<2191:DOTESJ>2.0.CO;2.

Han, W. Q., P. Webster, R. Lukas, and P. Hacker (2004), Impact of atmospheric intraseasonal variability in the Indian Ocean: Low-frequency rectification in equatorial surface current and transport, *J. Phys. Oceanogr.*, *34*(6), 1350–1372, doi:10.1175/1520-0485(2004)034<1350:IOAIVI>2.0.CO;2.

Jensen, T. G. (1993), Equatorial variability and resonance in a wind-driven Indian Ocean model, *J. Geophys. Res.*, *98*(C12), 22,533–22,552, doi:10.1029/93JC02565.

Knox, R. A. (1976), On a long series of measurements of Indian Ocean equatorial currents near Addu Atoll, *Deep-Sea Res.*, *23*, 211–221.

Le Blanc, J.-L., and J.-P. Boulanger (2001), Propagation and reflection of long equatorial waves in the Indian Ocean from TOPEX/POSEIDON data during the 1993–1998 period, *Clim. Dyn.*, *17*, 547–557, doi:10.1007/s003820000128.

Luyten, J. R., M. Fieux, and J. Gonella (1980), Equatorial currents in the western Indian Ocean, *Science*, *209*, 600–603, doi:10.1126/science.209.4456.600.

Masson, S., P. Delecluse, J.-P. Boulanger, and C. Menkes (2002), A model study of the seasonal variability and formation mechanism of the barrier layer in the eastern equatorial Indian Ocean, *J. Geophys. Res.*, *107*(C12), 8017, doi:10.1029/2001JC000832.

Masson, S., C. Menkes, P. Delecluse, and J.-P. Boulanger (2003), Impacts of salinity on the eastern Indian Ocean during the termination of the fall Wyrtki Jet, *J. Geophys. Res.*, *108*(C3), 3067, doi:10.1029/2001JC000833.

Masumoto, Y., H. Hase, Y. Kuroda, H. Matsuura, and K. Takeuchi (2005), Intraseasonal variability in the upper layer currents observed in the eastern equatorial Indian Ocean, *Geophys. Res. Lett.*, *32*, L02607, doi:10.1029/2004GL021896.

McPhaden, M. J. (1982), Variability in the central equatorial Indian Ocean. Part I: Ocean dynamics, *J. Mar. Res.*, *40*, 157–176.

Molinari, R. L., D. Olson, and G. Reverdin (1990), Surface current distributions in the tropical Indian Ocean derived from compilations of surface buoy trajectories, *J. Geophys. Res.*, *95*(C5), 7217–7238, doi:10.1029/JC095iC05p07217.

Murtugudde, R., and A. J. Busalacchi (1999), Interannual variability of the dynamics and thermodynamics of the tropical Indian Ocean, *J. Clim.*, *12*(8), 2300–2326, doi:10.1175/1520-0442(1999)012<2300:IVOTDA>2.0.CO;2.

Nagura, M., and M. J. McPhaden (2008), The dynamics of zonal current variations in the central equatorial Indian Ocean, *Geophys. Res. Lett.*, *35*, L23603, doi:10.1029/2008GL035961.

Niiler, P. P., N. A. Maximenko, G. G. Panteleev, T. Yamagata, and D. B. Olson (2003), Near-surface dynamical structure of the Kuroshio Extension, *J. Geophys. Res.*, *108*(C6), 3193, doi:10.1029/2002JC001461.

O'Brien, J. J., and H. E. Hurlburt (1974), Equatorial jet in the Indian Ocean: Theory, *Science*, *184*, 1075–1077, doi:10.1126/science.184.4141.1075.

Reppin, J., F. A. Schott, J. Fischer, and D. Quadfasel (1999), Equatorial currents and transports in the upper central Indian Ocean: Annual cycle and interannual variability, *J. Geophys. Res.*, *104*(C7), 15,495–15,514, doi:10.1029/1999JC900093.

Reverdin, G. (1985), Convergence in the equatorial surface jets of the Indian Ocean, *J. Geophys. Res.*, *90*(C6), 11,741–11,750, doi:10.1029/JC090iC06p11741.

Reverdin, G. (1987), The upper equatorial Inidan Ocean: The climatological seasonal cycle, *J. Phys. Oceanogr.*, *17*(7), 903–927, doi:10.1175/1520-0485(1987)017<0903:TUEIOT>2.0.CO;2.

Schott, F. A., and J. P. McCreary Jr. (2001), The monsoon circulation of the Indian Ocean, *Prog. Oceanogr.*, *51*, 1–123, doi:10.1016/S0079-6611(01)00083-0.

Vinayachandran, P. N., N. H. Saji, and T. Yamagata (1999), Response of the equatorial Indian Ocean to an unusual wind event during 1994, *Geophys. Res. Lett.*, *26*(11), 1613–1616, doi:10.1029/1999GL900179.

Wunsch, C. (1977), Response of an equatorial ocean to a periodic monsoon, *J. Phys. Oceanogr.*, *7*(4), 497–511, doi:10.1175/1520-0485(1977)007<0497:ROAEOT>2.0.CO;2.

Wyrtki, K. (1973), An equatorial jet in the Indian Ocean, *Science*, *181*, 262–264, doi:10.1126/science.181.4096.262.

Yuan, D. L., and W. Q. Han (2006), Roles of equatorial waves and western boundary reflection in the seasonal circulation of the equatorial Indian Ocean, *J. Phys. Oceanogr.*, *36*(5), 930–944, doi:10.1175/JPO2905.1.

L. Li and Y. Qiu, Third Institute of Oceanography, State Oceanic Administration, 178 Daxue Road, Xiamen 361005, China. (lili@tiosoa.cn)
W. Yu, First Institute of Oceanography, State Oceanic Administration, 6, Road Xian-Xia-Ling, Qingdao 266061, China.